

T Lymphocytes Orient against the Direction of Fluid Flow during LFA-1-Mediated Migration

Marie-Pierre Valignat,^{†*} Olivier Theodoly,^{††} Alexia Gucciardi,^{††} Nancy Hogg,[§] and Annemarie C. Lellouch^{††*}

[†]Laboratoire d'Adhésion Cellulaire et Inflammation, Aix Marseille Université, CNRS UMR7333, Marseille, France; ^{††}INSERM U1067, Marseille, France; and [§]Leukocyte Adhesion Laboratory, Cancer Research UK London, Research Institute, London, United Kingdom

ABSTRACT As they leave the blood stream and travel to lymph nodes or sites of inflammation, T lymphocytes are captured by the endothelium and migrate along the vascular wall to permissive sites of transmigration. These processes take place under the influence of hemodynamic shear stress; therefore, we investigated how migrational speed and directionality are influenced by variations in shear stress. We examined human effector T lymphocytes on intercellular adhesion molecule 1 (ICAM-1)-coated surfaces under the influence of shear stresses from 2 to 60 dyn.cm⁻². T lymphocytes were shown to respond to shear stress application by a rapid (30 s) and fully reversible orientation of their migration against the fluid flow without a change in migration speed. Primary T lymphocytes migrating on ICAM-1 in the presence of uniformly applied SDF-1 α were also found to migrate against the direction of shear flow. In sharp contrast, neutrophils migrating in the presence of uniformly applied fMLP and leukemic HSB2 T lymphocytes migrating on ICAM-1 alone oriented their migration downstream, with the direction of fluid flow. Our findings suggest that, in addition to biochemical cues, shear stress is a contributing factor to leukocyte migration directionality.

INTRODUCTION

The remarkable ability of leukocytes to leave the blood stream, cross the vascular endothelium, and enter tissue or organs is critical for both the innate and adaptive immune response. In the first line of defense, neutrophils and monocytes home to inflamed vascular endothelial sites and enter tissue to release antimicrobial molecules. During immunosurveillance, antigen-inexperienced, naïve T lymphocytes circulate constantly between the vasculature and lymph nodes, where they survey professional antigen-presenting cells for the presence of foreign antigen. If such antigen is encountered, the lymphocytes gain effector functions, such as cytokine secretion for helper CD4⁺ cells or acquisition of cytotoxic activities for CD8⁺ cells, and subsequently reenter the circulation to rapidly home to inflamed and/or infected tissues or organs (1). A common mechanism for leukocyte extravasation is currently defined as a multistep process that involves selectin-mediated capture to and rolling along the vascular wall, chemokine-mediated upregulation of the integrin family of adhesion receptors, firm adhesion, and finally either pericellular or transcellular migration across the vascular endothelium (2,3). After adhesion occurs, the polarized leukocytes migrate along the vascular wall in an integrin-dependent process called intraluminal crawling (4). This amoeboid form of motility involves the tightly integrated actions of integrin-mediated adhesion, Rho family GTPase-mediated actin polymerization events at the leading edge of the cell, and nonmuscle

myosin II-mediated contractility in the rear or uropod (5). Intraluminal crawling may allow the leukocyte to move away from its initial site of attachment and find permissive points of exit, such as at endothelial junctions (6). The quality, quantity, and spatial distribution of selectin ligands, integrin ligands, and chemokines are thought to provide directional cues to the migrating cells. However, in addition to these biochemical cues, leukocytes are also subjected to significant hemodynamic forces, in particular in the form of shear stress. The direction of shear stress is determined by the direction of flow, and its intensity depends upon blood flow rates and local vascular geometry.

During leukocyte extravasation, a number of processes are influenced by shear stress, such as leukocyte integrin activation, pseudopod formation, and transmigration (7–12). More specifically, shear stress can strengthen chemokine-triggered integrin adhesion of naïve T lymphocytes. It can also lead to more efficient transmigration with increased filopodia formation when naïve T lymphocytes transmigrate across the cellular endothelium in vitro (12–14). Taken together, these findings suggest that a variety of integrin-dependent and -independent cellular mechanisms that are also involved in intraluminal crawling may be sensitive to shear stress.

Intraluminal crawling was first observed in vivo in murine monocytes that patrolled the vascular endothelium, albeit with no apparent directional bias (15). Later in vivo studies of neutrophils showed that these leukocytes migrate preferentially in the direction of blood flow (6,16,17). In vitro migration experiments have also been performed on cultured human umbilical vein endothelial cells or on immobilized ligand, in which the relative contribution of specific $\beta 3$ or $\beta 2$ integrin ligands (e.g., platelet endothelial cell adhesion molecule 1 (PECAM-1) and intercellular

Submitted July 26, 2012, and accepted for publication December 5, 2012.

*Correspondence: marie-pierre.valignat@inserm.fr or annemarie.lellouch@inserm.fr

Alexia Gucciardi's present address is Beckman Coulter-Immunotech, Marseille, France.

Editor: Rick Horwitz.

© 2013 by the Biophysical Society
0006-3495/13/01/0322/10 \$2.00

<http://dx.doi.org/10.1016/j.bpj.2012.12.007>



adhesion molecule 1 (ICAM-1)) can be evaluated. Neutrophils express several integrins that are involved in motility, notably $\alpha v\beta 3$, which binds PECAM-1, and two $\beta 2$ integrins, lymphocyte-function-associated 1 (LFA-1; $\alpha L\beta 2$, CD11aCD18) and macrophage 1 (MAC-1; $\alpha M\beta 2$, CD11bCD18), both of which bind ICAM-1 (18). In the *in vitro* studies, neutrophils migrated randomly under static conditions and with a bias in the direction of fluid flow in a shear-stress-dependent fashion that was consistent with previous *in vivo* observations (19,20). Conversely, intravital imaging of rat CD4⁺ effector T lymphocytes bound to specialized cerebral structures, the leptomeningeal vessels, in an experimental autoimmune encephalitis model revealed that the lymphocyte migration was oriented preferentially against the direction of blood flow before transmigration (21). Furthermore, when mouse CD4⁺ effector lymphocytes were observed migrating on cultured mouse brain microvascular endothelial cells or on ICAM-1- or ICAM-2-immobilized ligand, the cells migrated randomly under static conditions and slightly against the direction of flow when shear stress was applied (22). These examples of T lymphocyte migration suggest that such leukocytes might respond differently to shear stress compared with neutrophils or monocytes. However, these previous studies on T lymphocytes were limited to observations in the pathological context of autoimmune encephalitis in mice. Moreover, they only investigated activated effector lymphocytes under limited shear stress conditions (e.g., 1.5 dyn.cm^{-2}) that were lower than the shear stress rates known to exist in postcapillary venules. It also remains to be determined whether the lymphocyte response to shear stress depends on the lymphocyte activation state or the level of shear imposed on the migrating cell.

The shear stress of interest in this study relates to the conditions encountered in the postcapillary venules, where leukocyte extravasation predominantly takes place. Moreover, naïve and central memory T lymphocytes enter lymph nodes by migrating across specialized high endothelial venules. Although it is difficult to characterize hydrodynamic properties in the highly confined microenvironment of the postcapillary venules, several studies that focused on the microvasculature, in deep organs of mammals or in human conjunctiva and retina, yielded consistent orders of magnitudes. According to these studies, the diameters of capillary venules range between 15 and 30 μm (23,24), and local shear stresses span between 3 dyn.cm^{-2} (24,25) and 10 dyn.cm^{-2} (26,27), with maximum values reaching 25–30 dyn.cm^{-2} (27,28). These values establish the range of shear stress that should be reproduced for *in vitro* experiments intending to probe physiological mechanisms.

To gain a more thorough understanding of how T lymphocytes might respond to variations in shear stress, we undertook a systematic study of the speed and directionality of human T lymphocytes migrating on ICAM-1-immobilized microchannels under physiological shear stress rates

between 0 and 12 dyn.cm^{-2} . To determine the influence of the lymphocyte activation state, we examined both freshly isolated human T lymphocytes, which for simplicity we will refer to as primary T lymphocytes, and T lymphocytes activated *in vitro* and subsequently cultivated with interleukin 2 (IL-2), which we will refer to as effector T lymphocytes. We also investigated the behavior of freshly isolated human neutrophils and HSB2 cells, a T lymphocyte line derived from an aggressive T acute lymphoblastic leukemia (T-ALL). In our assay, each cell type was provided with the minimal necessary elements to sustain migration, namely, a homogeneous surface presentation of ICAM-1-Fc in combination with stromal-cell-derived factor 1 α (SDF-1 α) or N-formyl-methionyl-leucyl-phenylalanine (fMLP) for the primary T cells and neutrophils, respectively, or ICAM-1-Fc alone for the effector T lymphocytes or HSB2 cells. Under these conditions, we found sharply contrasted behaviors between different cells when shear stress was applied. Neutrophils and HSB2 T lymphocytes migrated systematically in the direction of fluid flow, whereas both the primary and the effector human T lymphocytes migrated against the direction of fluid flow. Directional bias increased with shear stress intensity, whereas linear speed is never affected by the action of flow. Changes in directional bias versus flow were found to occur within a few tens of seconds and were completely reversible. Our findings suggest that, in addition to biochemical cues, shear stress is a contributing factor to leukocyte migration directionality, and that different leukocytes may respond to their hemodynamic environment differently.

MATERIALS AND METHODS

Cells and reagents

Whole blood from healthy adult donors was obtained from the *Établissement Français du Sang*. Peripheral blood mononuclear cells (PBMCs) were recovered from the interface of a Ficoll-Paque PLUS (GE Healthcare, Pittsburgh, PA) gradient. The PBMCs were stimulated with either 10 $\mu\text{g/mL}$ phytohemagglutinin-L (PHA-L; Roche Diagnostics, Indianapolis, IN) or anti-CD3/anti-CD28 Dynabeads (Invitrogen, Carlsbad, CA) according to the manufacturer's instructions. PBMCs were subsequently cultivated in Roswell Park Memorial Institute Medium (RPMI) 1640 supplemented with 25 mM HEPES and 25 mM GlutaMax (Gibco, Carlsbad, CA), 10% fetal calf serum (FCS; Lonza, Basel, Switzerland) at 37°C, 5% CO₂ in the presence of IL-2 (50 ng/ml; Miltenyi Biotec, Auburn, CA) and used 7–10 days after stimulation. At the time of use, the cells were >95% positive for pan-T lymphocyte marker CD3 ϵ and negative for T lymphocyte activation marker CD69 as judged by flow cytometry. To isolate naïve T lymphocytes, freshly isolated PBMCs were subjected to negative selection using the Pan T lymphocyte isolation kit (Miltenyi Biotec). Cells were used in migration experiments within 24 h after they were isolated. Neutrophils were isolated from fresh blood samples by centrifugation in lymphocyte separation medium (Eurobio, Les Ulis, France). Residual red blood cells were lysed by treatment with 0.14 M NH₄Cl. Neutrophils were then maintained at 37°C in a humidified atmosphere containing 5% CO₂, and used in experiments within 2–3 h. The HSB2 human T lymphocyte line was cultivated in RPMI, 10% FCS supplemented as for the PBMCs. Fluorescent conjugates of anti-CD3 ϵ (UCHT1),

anti-CD4 (OKT4), anti-CD8 (HIT8a), anti-CD11a (HI111), CD11b (ICRF44), and anti-CD18 (TS1/18) were obtained from Biolegend (San Diego, CA). APC-anti-CD69 was obtained from BD Biosciences (Franklin Lakes, NJ). The blocking antibodies for CD11a (HI111) and CD11b (ICRF44), as well as the isotype control, were obtained from Biolegend.

Flow channel preparation

Ibidi channels IV^{0.4} (Ibidi GMBH, Martinsreid, Germany) were coated overnight at 4°C with 10 µg/ml human ICAM-1-Fc (R&D Systems, Minneapolis, MN) in PBS (Gibco) with or without either SDF-1α (R&D Systems) or fMLP (Sigma-Aldrich, St. Louis, MO). Channels were subsequently blocked with a solution containing 2.5% bovine serum albumin (w/v; Axday, Dardilly, France) and 2.5% Pluronic acid F-108 (w/v; BASF, Ludwigshafen, Germany) in PBS for 30 min at room temperature. Channels were rinsed three times with Hank's buffered saline solution supplemented with 5 mM MgCl₂, 5 mM CaCl₂, and 5 mM Hepes. Cells were added in complete culture medium at densities of $\sim 2 \times 10^6$ /ml and allowed to equilibrate for 10 min at 37°C before image acquisition was initiated.

Migration assays under flow

Cells in the flow chambers were observed at 37°C with a Zeiss Z1 automated microscope (Carl Zeiss, Oberkachen, Germany) equipped with a CoolSnap HQ CCD camera (Photometrics, Tucson, AZ) and piloted by µManager (29). Flow of prewarmed and CO₂ equilibrated culture media through the flow chamber was controlled using an Ibidi pump system (Ibidi GMBH, Martinsreid, Germany). Bright-field images (Plan-Apochromat 20x/0.8 objective) were collected every 10 s over the time frame indicated. The field of view represents $870 \times 650 \mu\text{m}^2$.

Cell tracking and data analysis

An image-processing program was developed in house to automatically detect and track the migrating cells using MATLAB software (The MathWorks, Natick, MA). The principal steps of the program are as follows: 1), performing automated image quality enhancement using background division and intensity normalization; 2), thresholding and binarizing the images to distinguish cells from the background; and 3), identifying and numbering cells in the first image and following them in the next image (Fig. 1 A). Further steps include 4), writing the output, which contains the coordinates and time information for each identified cell; and 5), displaying the identified trajectories on the first frame (Fig. 1 B) or displaying all of the trajectories starting with initial coordinates (0,0) on an XY plot (Fig. 1 C). In all flow experiments, the flow is directed from the top to the bottom of the images presented here (Fig. 1, C and D). A Y forward migration index, Y_{FMI} is calculated by dividing the distance the cells travel in the Y axis direction by the cells' contour length, $Y_{i,end}/d_{i,accum}$. This Y_{FMI} index gives an indication of the amount of movement that is in the direction of flow versus the total trajectory, and is equivalent to the chemotactic index that is usually used to quantify the migration direction relative to gradients of chemotactic factors (30). The average speed of a cell, V , is calculated based on its total trajectory as the ratio between the contour length $d_{i,accum}$ and the corresponding time of migration. All calculations were performed at least in triplicate for each cell type and >10 times for the effector T lymphocytes.

RESULTS

Adhesion versus shear stress

Cells were introduced into a channel that was previously coated with either ICAM-1-Fc alone for effector T lympho-

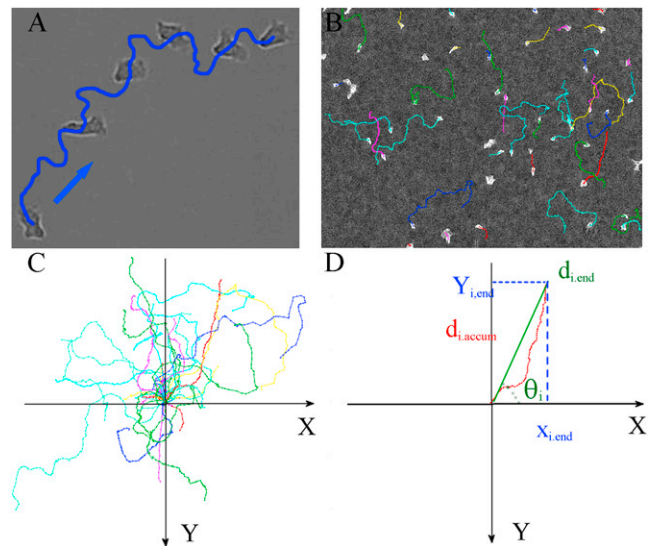


FIGURE 1 Cell tracking and data analysis. (A) Bright-field images of the migration of a single cell shown at different time points (0 s, 270 s, 400 s, 500 s, 580 s, and 650 s). (B) Bright-field images of T lymphocytes and their trajectories recorded during 16 min. (C) Cell trajectories with initial coordinates (0,0). (D) Parameter definitions. The initial coordinates of the cell are (0,0). Flow is directed from top to bottom, $Y_{i,end}$ is the distance the cell number i traversed in the direction of flow, and $d_{i,accum}$ is the contour length of the cell trajectory. We define the Y forward migration index, or Y_{FMI} , as $Y_{i,end}/d_{i,accum}$, which is positive if the net translation is in the direction of the flow. θ_i is defined as the angle between the X axis and the axis joining the initial and final positions of the cell number i . It is counted positively in counterclockwise rotation.

cytes and HSB2 cells, ICAM-1-Fc in combination with the chemokine SDF-1α for primary T lymphocytes, or ICAM-1-Fc in combination with the stimulant fMLP for neutrophils. After injection and a resting time of 10 min without flow, the percentage of cells that adhered to and migrated on the surface was ~ 50 –80%. These migrating cells had a polarized and flattened shape composed of a lamellipodia at the front and a uropod in the rear, whereas the nonadherent cells maintained a spherical shape. The nonadherent cells were easily washed away by application of a gentle flow at $2 \text{ dyn}\cdot\text{cm}^{-2}$. To estimate the adhesion strength of migrating cells under stronger flow, we counted the numbers of cells that remained adhered after 16 min under a shear stress of $8 \text{ dyn}\cdot\text{cm}^{-2}$. The average ratio was found at 22%, 68%, and 65% for primary, effector, and HSB2 T lymphocytes, respectively, and 90% for neutrophils. Adhesion strength was clearly lower for primary T lymphocytes than for neutrophils and effector and HSB2 T lymphocytes.

T lymphocytes migrate upstream

Leukocytes leave the vasculature at sites of infection or inflammation via transmigration through the endothelium of postcapillary venules, where shear stresses average 5 – $10 \text{ dyn}\cdot\text{cm}^{-2}$. Therefore, we first applied a shear stress of $8 \text{ dyn}\cdot\text{cm}^{-2}$ to effector T lymphocytes and the HSB2 T

lymphocyte line migrating on ICAM-1-Fc alone, and primary T lymphocytes and neutrophils migrating on ICAM-1-Fc coimmobilized with SDF1- α and fMLP, respectively. We collected images every 10 s for 16 min and tracked the individual cell trajectories. There was no migrational difference between the effector T lymphocytes cells generated by the lectin PHA or by anti-CD3/anti-CD28-coated beads (data not shown); therefore, in the following text, all effector T lymphocytes correspond to PHA-activated cells.

Under static conditions, the migration direction was random (i.e., without directional bias) for all four cell types, as shown by the angle histograms (Fig. 2, upper panel). However, the directional migration was strongly biased by the imposition of flow. Under a shear stress of 8 dyn.cm^{-2} , we observe two markedly distinct behaviors between the different cell types: primary and effector T lymphocytes migrate against the direction of flow, whereas the HSB2 T lymphocytes and neutrophils migrate in the direction of flow (Fig. 2, lower panel; see also Movie S1, Movie S3, Movie S4, and Movie S5 in the Supporting Material). Fig. 2 also reveals that the distribution of angles is extremely narrow for effector and HSB2 T lymphocytes, meaning that the trajectories of the cells are almost straight, whereas the distributions for neutrophils and naïve T lymphocytes are broader, indicating that their trajectories are more sinuous. Finally, it is worth noting that the cell migration directionality is essentially imposed by the flow to each individual cell for T lymphocytes and HSB2 T lymphocytes. The lower hemisphere for effector T lymphocytes and the higher hemisphere for HSB2 T lymphocyte in Fig. 2 (lower panel) are

almost empty, with $>98\%$ of cells having their direction imposed by flow. Such a behavior characterizes a very homogeneous and efficient response of cells to flow.

Downstream migration of neutrophils is supported by either LFA-1 or MAC-1

Unlike T lymphocytes, neutrophils express two $\beta 2$ -integrins that can bind ICAM-1: MAC-1 ($\alpha M\beta 2$, CD11bCD18) and LFA-1 ($\alpha L\beta 2$, CD11aCD18). One might reasonably question whether the presence of MAC-1 contributes to the difference in directionality between the neutrophils and the two healthy T lymphocyte populations as they migrate on ICAM-1. To explore whether the presence of MAC-1 is required for the downstream migrational behavior of neutrophils, we first employed flow cytometry to examine the expression of αL (CD11a), αM (CD11b), and $\beta 2$ (CD18) on primary, effector, and HSB2 T lymphocytes, as well as on neutrophils. As expected, neutrophils expressed both αM and αL along with $\beta 2$, confirming the presence of both LFA-1 and MAC-1 (Fig. 3 A). Conversely, no MAC-1 expression could be detected on any of the three T lymphocyte populations, including the leukemic HSB2 cells, which also migrated with the direction of flow. To determine whether MAC-1 was required to maintain the downstream orientation of neutrophils migrating on ICAM-1 under shear stress, we preincubated neutrophils with $50 \mu\text{g/mL}$ blocking antibodies for either αM (CD11b) or αL (CD11a). In the presence of either blocking antibody, adhesion was weakened (the fraction of cells at 8 dyn.cm^{-2} that remained adherent was reduced by a factor

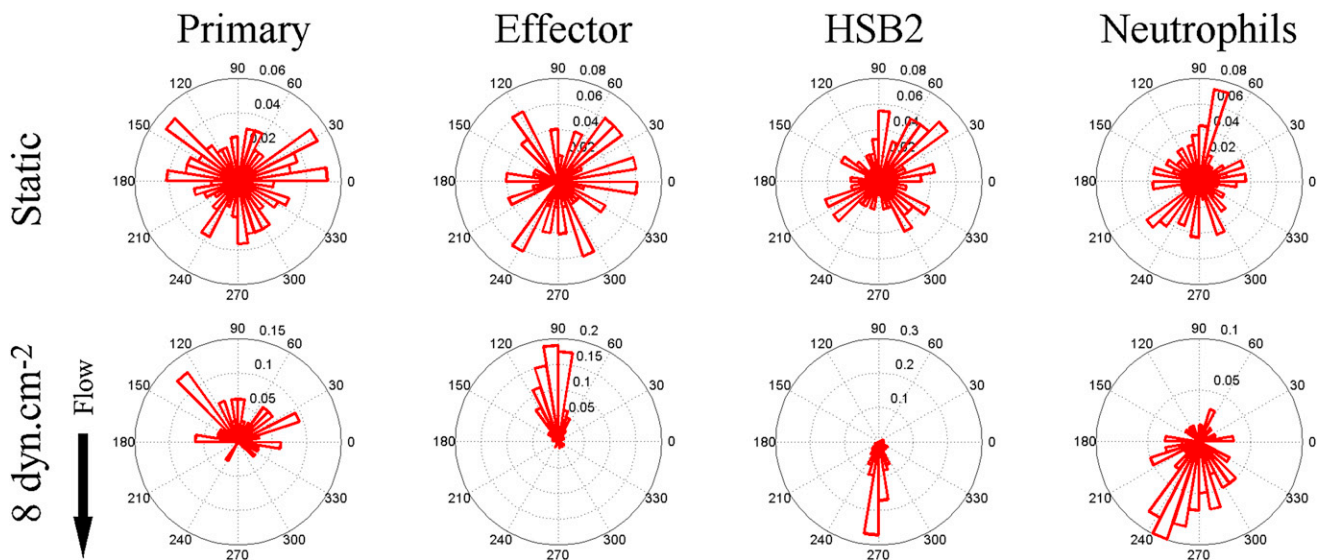


FIGURE 2 Angle histogram for one representative experiment in four different leukocyte cell populations (primary T cell, effector T cells, HSB2 T cells, and neutrophils) in static (upper panels) and flow (lower panels) conditions showing the distribution of θ in ≤ 40 angle bins. The length of each bin reflects the fraction of cells with a given angle that fall within a group. Under the flow condition, the shear stress was set to a value of 8 dyn.cm^{-2} and the direction of the flow was along the Y axis from top to bottom, as indicated by the arrow. The numbers of cells analyzed were respectively 192, 234, 148, and 134 in the static condition and 23, 73, 93, and 60 under the flow condition for primary T cells, effector T cells, HSB2 T cells, and neutrophils.

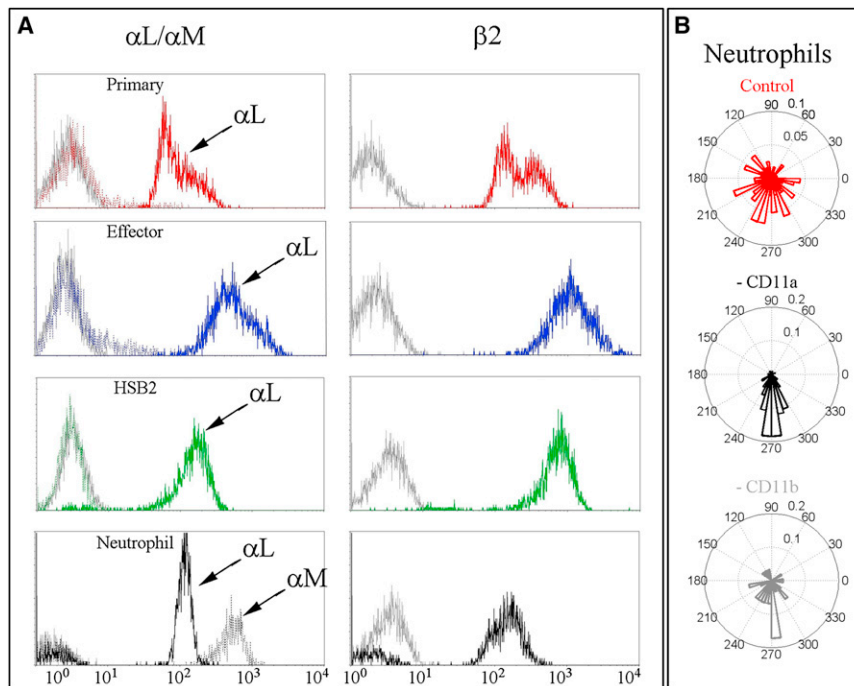


FIGURE 3 Expression of LFA-1 and MAC-1 on T lymphocytes and neutrophils. (A) The expression levels of the two integrin α subunits, $\alpha L/CD11a$ (solid colored lines) and $\alpha M/CD11b$ (dotted colored lines) are depicted in the left panels, and the integrin $\beta 2$ chain is shown in the right panels (solid colored line) for primary T lymphocytes (red), effector T lymphocytes (blue), HSB2 T cell line (green), and neutrophils (black). All negative controls are depicted with solid gray lines. (B) Angle histograms of a representative experiment of neutrophils migrating at 8 dyn.cm^{-2} after pretreatment with an isotype control (upper histogram) or $50 \text{ }\mu\text{g/mL}$ blocking antibodies directed against either CD11a (middle histogram) or CD11b (bottom histogram). Histograms represent tracking of 117, 50, and 31 cells for the control, anti-CD11a, and anti-CD11b, respectively.

of 2 with blocking antibodies as compared with controls), but the Y_{FMI} remained markedly positive in both cases (Fig. 3 B). These findings suggest that the direction of migration on ICAM-1 with respect to the fluid flow of neutrophils is maintained by either form of $\beta 2$ integrin (i.e., LFA-1 or MAC-1) that is present at the cell surface, and therefore the presence of MAC-1 is not a critical factor responsible for the downstream orientation observed for neutrophils.

Directionality, but not speed, is dependent on shear stress rate

Shear stresses in postcapillary venules can be as high as $25\text{--}30 \text{ dyn.cm}^{-2}$ (24,27,28); however, most studies that used in vitro models for leukocyte migration employed relatively lower shear stress rates, on the order of $0.5\text{--}5 \text{ dyn.cm}^{-2}$ (12,13,22). To more fully explore how migration directionality and speed are influenced by variations in the hemodynamic microenvironment, we next examined the effect of the rate of shear stress in the range of $0\text{--}12 \text{ dyn.cm}^{-2}$. After the initial 10 min resting period, shear stress was sequentially increased stepwise every 100 images (16 min) from 2 dyn.cm^{-2} to 4, 8, and 12 dyn.cm^{-2} . The migration index along the Y axis, Y_{FMI} , averaged over the number of cells, is illustrated for one representative experiment in each of the four different cell types in Fig. 4 A, and data accumulated from four independent experiments with the effector T lymphocytes are shown in Fig. 4 C. Y_{FMI} is an indicator of movement efficiency along the axis of flow direction. Under the initial static conditions (shear stress of 0 dyn.cm^{-2}), the

Y_{FMI} of each cell type was null, meaning that migration was random, i.e., lacking directional bias. At the lowest shear stress of 2 dyn.cm^{-2} employed in this study, the average Y_{FMI} of -0.2 for both primary and effector T lymphocyte populations reveals a significant directional bias against the direction of fluid flow. For higher shear stresses, the directional bias for primary T lymphocyte migration remained stable, whereas the Y_{FMI} of effector T lymphocytes decreased further down to -0.7 for a shear stress rate of 12 dyn.cm^{-2} . In contrast, the HSB2 T lymphocytes and neutrophils always migrated with a positive Y_{FMI} that increased up to a maximal value of 0.6. The HSB2 T lymphocyte seemed to be particularly sensitive to the effect of flow: Y_{FMI} was already as high as 0.5 at 2 dyn.cm^{-2} , which is the strongest response observed for all of the cell types. The average cell speed is illustrated for representative experiments in each of the four different cell types in Fig. 4 B, and data accumulated from four independent experiments with the effector T lymphocytes are shown in Fig. 4 D. Under our experimental conditions, the average migration speed was between 15 and $21 \text{ }\mu\text{m/min}$ for all leukocyte populations, in accordance with published results (3). Strikingly, shear stresses of up to 12 dyn.cm^{-2} had hardly any influence on the average cell speed, independently of the cell type and cell migration direction versus flow.

To further test the migration mechanisms under flow beyond standard physiological conditions, we performed a series of experiments focusing on the effector T lymphocytes at rates as high as 60 dyn.cm^{-2} . Fig. 5 A shows that cell detachment increased significantly with shear stress until $<10\%$ of the cells that initially were adherent at

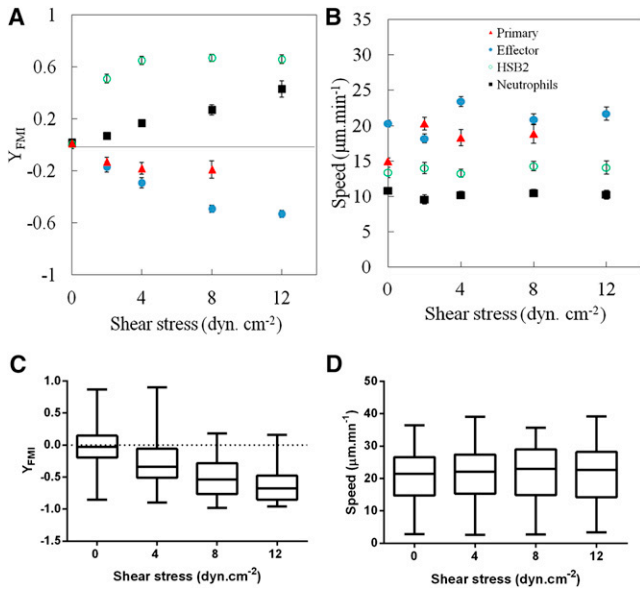


FIGURE 4 Leukocyte response to shear stress rate. (A and B) Y_{FMI} (A) and speed (B) for a representative experiment in four different leukocyte cell populations (primary T cells (triangles), effector T cells (solid circles), HSB2 T cells (open circles), and neutrophils (squares)). Number of cells analyzed: $N > 50$ except for primary cells at $\sigma = 8 \text{ dyn.cm}^{-2}$, where $N = 23$. Data are mean \pm SE. (C and D) Y_{FMI} (C) and speed (D) were calculated for four independent experiments in effector T cells. Box-and-whisker plots show the smallest and largest, lower and upper quartiles, and median observations. Number of cells analyzed: $N = 100\text{--}300$. Data for Y_{FMI} in the absence of flow are not significantly different from zero. One-way ANOVA followed by the Tukey multiple-comparison test confirmed the existence of significant differences in Y_{FMI} for different values of shear stress (all p-values < 0.0001 , except between 8 and 12 dyn.cm^{-2} , for which the difference is not significant ($p > 0.05$)). One-way ANOVA followed by the Tukey multiple-comparison test confirmed the absence of significant differences in speed for different values of shear stress (all p-values > 0.05).

2 dyn.cm^{-2} remained attached at 60 dyn.cm^{-2} . Interestingly, at low shear stress, the proportion of adherent but nonmotile cells was negligible, whereas these same nonmotile cells accounted for a significant proportion of the total population as shear stresses increased, reaching 40% at 60 dyn.cm^{-2} . This observation suggests that nonmotile cells are immobile due to a particularly high adhesion, whereas motile cells are less strongly adhered and more sensitive to the detaching effect of flow. Because this finding revealed that the cell populations in a given experiment were significantly different at low and high shear stress, we adapted the data analysis accordingly. For cell migration orientation at high shear stress, we first identified the cells that were nonmotile under low shear stress and discarded those cells from the analysis of high-shear-stress data. The data in Fig. 5 B reveal the complete dependence of Y_{FMI} versus shear stress. Y_{FMI} decreases strongly for shear stress lower than 20 dyn.cm^{-2} and more weakly for larger shear stress, up to a minimum value of -0.9 at 60 dyn.cm^{-2} (see Movie S1). Concerning our analysis of cell migration speed versus shear stress, the difference in cell populations at low and

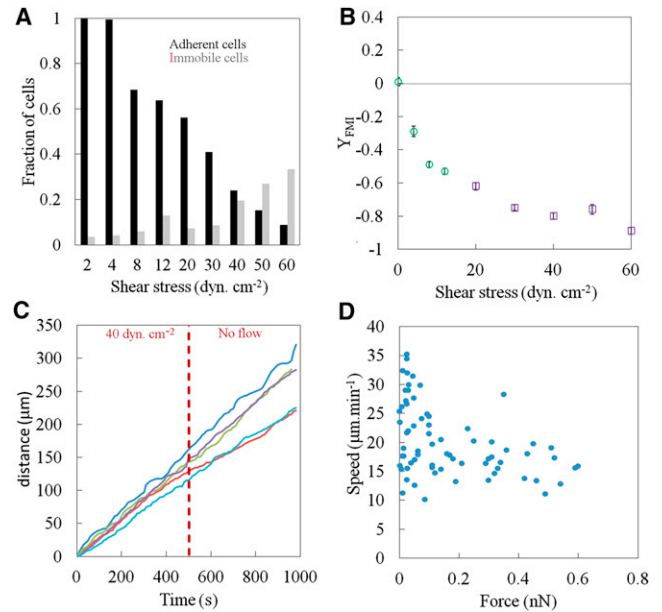


FIGURE 5 Effector T lymphocytes at high shear stress. (A) Evolution as a function of the shear stress of the fraction of adherent cells relative to the number of cells that initially adhered in the absence of flow (black bars), and of the fraction of immobile cells among adherent cells at a given shear stress (gray bars). Initial cell numbers: $N = 150$. (B) Y_{FMI} versus shear stress. Green circles correspond to the average Y_{FMI} of all cells at a given shear stress, and violet circles indicate the average Y_{FMI} of the remaining migrating cells only. Number of cells analyzed ranged between 171 in static conditions and 16 at highest shear stress. Data are mean \pm SE. (C) Cumulative distance versus time of individual cells (each color corresponds to a different unique cell) with a shear stress of 40 dyn.cm^{-2} between 0 and 500 s, and no flow between 500 and 1000 s. (D) Average speed of individual cells as a function of the total force F exerted by the flow, where F is estimated as the product of the projected cell area S_p of individual cells and the applied shear stress σ , $F = S_p \times \sigma$.

high shear stress, combined with the large distribution of cell speed in a population, makes it difficult to precisely detect a potential effect on data that have been averaged over a population. We therefore examined the behavior of individual cells, tracking their trajectories for 500 s at $\sigma = 40 \text{ dyn.cm}^{-2}$ and then for an additional 500 s at $\sigma = 0 \text{ dyn.cm}^{-2}$. In Fig. 5 C, we report the total distance covered by single cells versus time. There is no detectable change of slope when the shear stress is cut, which clearly shows that shear stresses up to 40 dyn.cm^{-2} have no influence on migration speed. Finally, cells within a given population have different surface areas and therefore experience different degrees of force for a given applied shear stress. Using the projected area of individual cells, S_p , we report in Fig. 5 D the speed of individual cells versus the effective force, $F = S_p \times \sigma$, experienced by cells for a shear stress range $\sigma = 0\text{--}60 \text{ dyn.cm}^{-2}$. We find the range of force experienced by cells to be between 0 and 0.6 nN. It is interesting to note that the more-rapid cells, with speeds in the range of $20\text{--}35 \mu\text{m.mn}^{-1}$, are only present at low force because they correspond to cells that detach first when the shear stress is

increased. This further supports the idea that cell speed in our experiments is anticorrelated with adhesion strength. However, the majority of cells with speeds in the range of $15\text{--}20\ \mu\text{m}\cdot\text{mn}^{-1}$ remain attached under shear and keep a constant speed throughout the whole range of forces applied ($0\text{--}0.6\ \text{nN}$).

The directional influence of shear stress is rapid, reversible, and robust

Having established that human leukocytes had individual responses to shear stress, we wished to characterize the kinetics and reversibility of the phenomenon. We applied a series of sequential cycles of 16 min with and without an applied shear stress of $8\ \text{dyn}\cdot\text{cm}^{-2}$ to effector T lymphocytes (see [Movie S2](#)). Images were collected every 10 s, and the average Y_{FMI} and average speed of the population of cells in each image were calculated over 10 images and plotted against time. The transitions between random migration during the periods without flow (Y_{FMI} close to zero) and highly directed motion during application of flow ($Y_{FMI} \sim -0.6$) occurred in $\sim 30\ \text{s}$ ([Fig. 6 A](#)). The behavior of cells in a given population showed little change between the five consecutive cycles of an experiment.

Concerning the average cell speed, we found only a minor modulation of speed when the shear stress conditions were alternated with no shear, and a slight increase in cell speed against the flow during periods of applied shear stress ([Fig. 6 B](#)). These results clearly demonstrate that lymphocytes orient their migration rapidly and reversibly as a response to shear stress modulations without a change in speed.

DISCUSSION

In the study reported here, we performed a systematic analysis of the migration of primary and effector human T lymphocytes, a leukemic T lymphocyte cell line, and neutrophils on the LFA-1 integrin ligand ICAM-1 with and without minimal essential chemokines and in the presence of a wide range of physiological rates of shear stress,

such as might be encountered in the circulation. Our goal was to determine which aspect of the migrational process (i.e., speed, directionality, or orientation with respect to fluid flow) is most influenced by changes in local shear stress, and thereby clarify how leukocytes react to their hydrodynamic environment.

In the course of our experiments, we found that the speed of migration of all four cell types examined was largely independent of the applied shear stress, which is consistent with the observations of Rainger et al. (19). This conclusion was valid regardless of whether the cells migrated with or against the direction of fluid flow. In models of integrin-dependent cell migration, the cell speed has been shown to depend on three variables: integrin levels, ligand levels, and integrin-ligand affinity (31). In our experiments on ICAM-1-coated surfaces, the types and levels of ligands were fixed. The integrin expression levels differed from one type of cell to the other but remained constant for each cell type during the course of an experiment. Among the three variables of this model, only the integrin-ligand affinity may change for a given cell type and hence modulate the cell speed. The fact that cell speed is independent of shear stress suggests either that there is no modulation of integrin-ligand affinity, which is not consistent with some other studies (8), or that speed regulation is not driven only by integrin-ligand affinity modulations, at least in our experimental conditions. The question remains open as to why shear flow has little or no influence on the speed of crawling cells. An explanation may be found in a comparison of the force applied by the flow to the cell with the force developed by the cell motility machinery. In our experiments, the maximum force experienced by individual cells was estimated at $\sim 0.6\ \text{nN}$, which corresponds to a shear stress $\sigma = 60\ \text{dyn}\cdot\text{cm}^{-2}$ exerted on a typical cell surface $S_p = 100\ \mu\text{m}^2$. On the other hand, the force that drives cell movement is produced by the advancing lamellipodium under the action of actin network polymerization, which pushes the lamellipodium front parallel to the surface. Abraham et al. (32) combined the density of growing actin filaments at the lamellipodium margin and the maximum force obtained via actin assembly to estimate the total force

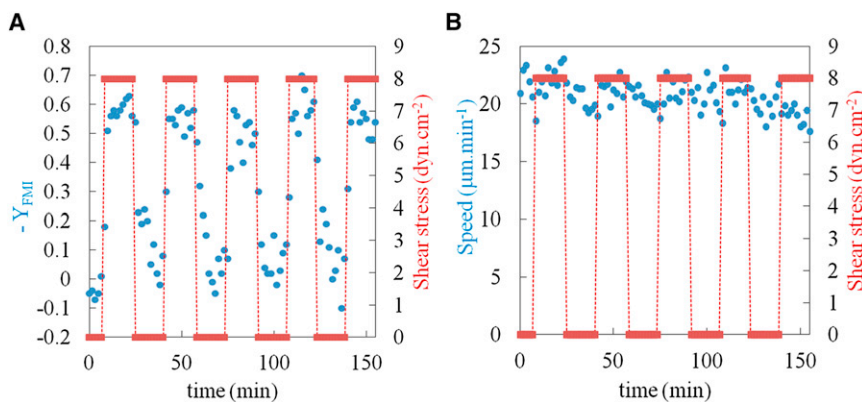


FIGURE 6 Effector T lymphocyte response to a periodic square wave shear stress. (A and B) Y_{FMI} (A) and speed (B) are reported (circles) versus the time in response to a periodic square wave of length 33 min and of shear stress intensity of $8\ \text{dyn}\cdot\text{cm}^{-2}$ (bars). The speed and Y_{FMI} of 10 frames were calculated (100 s).

exerted by the lamellipodium of a moving fibroblast to be on the order of a few nanonewtons. Marcy et al. (33) obtained direct force measurements in vitro on actin tails pushing 2 μm diameter beads, and found that the stall force was ~ 5 nN, confirming that actin can produce forces in the range of nanonewtons (33). These estimates clearly show that the force imposed by fluid flow is at least one order of magnitude lower than the lamellipodium growing force, which could explain why no passive acceleration or deceleration of cell movement was detected in our experiments. Taken together, our results suggest that the cell movement, once initiated, is powered by a strong motor (actin polymerization) and mediated via weakly adhesive bonds coupling cell-bound LFA-1 with ICAM-1. The fluid flow cannot reduce cell speed, which is imposed by the powerful cytoskeletal machinery, but it can detach weakly adhered cells.

In contrast to the speed of migration, it is clear that the direction of migration of each cell type tested under its particular migratory condition is influenced dramatically by shear stress. Moreover, two distinct and diametrically opposed responses were observed with respect to the direction of the fluid flow. The primary and effector T lymphocytes migrated against the direction of fluid flow, whereas the leukemic HSB2 cells and neutrophils migrated with the direction of fluid flow. In studies of both T lymphocytes and neutrophils, the shear stress-directed migration required specific integrin-ligand interactions. Murine effector CD4+ T lymphocytes oriented their migration on ICAM-1, but not on ICAM-2 and VCAM-1, which are expressed on murine blood-brain endothelial monolayers, suggesting a specific role of signaling events supported or initiated by LFA-1 binding to ICAM-1 (22). By the same token, early work on neutrophil migration suggested that although $\beta 2$ integrins are necessary for firm neutrophil adhesion and motility, directed motility requires an additional contribution from either integrin $\alpha v\beta 3$ or homophilic binding to PECAM-1 (19). However, our work and that of Smith et al. (20) demonstrate that neutrophils can migrate and orient their migration in the direction of fluid flow on uniform surfaces of ICAM-1, implying that the binding of either $\beta 2$ integrin, LFA-1, or MAC-1 to ICAM-1 is sufficient to induce shear-stress-oriented migration. Our results from blocking-antibody experiments support this hypothesis for neutrophils.

Smith et al. (20) proposed a mechanism to explain the directionality of neutrophils under flow, where nascent lamellipodia reorient in the direction of fluid flow in the brief periods during which protrusions are not attached. Within this model, directed movement of neutrophils under flow takes place passively without a mechanosensing mechanism. Although a passive alignment of protruding lamellipodia with fluid flow is a plausible explanation for neutrophils, it is difficult to reconcile with the upstream migration orientation of T lymphocytes. This point raises

the possibility that another mechanism may be involved in the migration orientation of lymphocytes. Other findings in the literature support the existence of an active mechanotransduction mechanism for orientation of leukocytes under flow. Phillipson et al. (16) reported that in the absence of expression of Vav1, murine neutrophils showed an exaggerated orientation in the direction of fluid flow when migrating on a mixed integrin-ligand surface. Because Vav1 is a guanine exchange factor for Rho family GTPases known to link integrins to Rac activities, this finding suggests that integrin-mediated signaling may regulate shear flow orientation (16). However, one might argue that in the absence of Vav-1, the adhesion strength of neutrophils is lessened and the action of flow induces a more efficient (albeit passive) drift of cells in the direction of flow. Hence, the findings of Phillipson et al. do not definitely demonstrate the existence of a mechanotransduction signaling process for regulating directionality. Like T lymphocytes, *Dictyostelium* cells migrate with an amoeboid behavior against fluid flow. Dalous et al. (34) examined actin-myosin reorganization during cell polarity reversal in *Dictyostelium* cells under both mechanical and chemical stimulation. Interestingly, they found similar patterns of front-to-tail interconversion upon reversion of either chemoattractant gradients or shear stress direction. This finding suggests that the mechanical response, like the chemical response, involves active detection and transduction processes. In addition, they found a characteristic time of polarity reversal of ~ 30 s for *Dictyostelium* cells, which is very similar to the characteristic response time to changes in flow direction that we found for T lymphocytes. Taken together, these results support the possible existence of a mechanotransduction mechanism. There are also recent examples of cells moving in opposition to a force that was applied locally on individual cells with magnetic (35) or optical (36) tweezers. Weber et al. (36) demonstrated that force applied on one side of a *Xenopus* mesendodermal cell caused the generation of actin-based protrusions opposite to and away from the direction of pulling on the other side of the cell. The mechanisms underlying this phenomenon have not been fully elucidated, but the authors demonstrated that the sites of force application were coupled by keratin intermediate filaments. It is tempting to speculate that shear stress experienced by the T lymphocyte may also trigger signals to or changes in the direction of the cytoskeletal machinery in the opposite direction of the experienced force.

Our findings regarding the influence of fluid flow on leukocyte migration demonstrate that the speed of migration is not affected by shear flow, which may be explained by the fact that the overall shear stress force exerted on the cell is negligible compared with the force generated by the advancing lamellipodium. However, the direction of migration of both primary and effector T lymphocytes is rapidly and reversibly modified. Furthermore, primary and effector human T lymphocytes, migrating with or without the

presence of SDF-1 α , respectively, respond to hydrodynamic stress in a manner distinct from that of neutrophils and the leukemic T lymphocyte line HSB2, by preferentially orienting themselves against rather than with the direction of fluid flow. Although it is not yet possible to conclude whether this behavior is a passive response to hydrodynamic forces or involves a specific mechanotransduction process, which may or may not require additional input from chemokines in some cases, these results raise fundamental questions about the role of the hemodynamic environment during directed intraluminal leukocyte migration. Future studies of the mechanisms involved in the lymphocyte response to shear stress will be influenced by published works describing the effect of shear stress on the vascular endothelium, which involves other membrane-bound protein activities such as stretch-activated calcium channels, expression of growth factor receptors, and nitric oxide synthase (7). Also relevant is endothelial wound healing, in which fluid flow has been shown to induce an asymmetric inhibition of Rac activity that leads to preferential protrusion in the direction of flow (37). Finally, it is of interest to know whether the altered directional response to shear stress observed for the leukemic HSB2 cells also applies to other malignant T lymphocyte populations. In conclusion, numerous pathologies involve abnormal vascular architectures, notably in the neovascularization of solid tumors or tissues specific to certain autoimmune disorders, which in turn give rise to atypical local hemodynamic properties (38). Understanding how T lymphocytes are influenced by both their hemodynamic and biochemical environments will shed light on how these important players in the immune system negotiate pathological vascular modifications.

SUPPORTING MATERIAL

Five movies and their legends are available at [http://www.biophysj.org/biophysj/supplemental/S0006-3495\(12\)05118-1](http://www.biophysj.org/biophysj/supplemental/S0006-3495(12)05118-1).

We thank Anne Pierres, Pascal Preira, and Sophie Cadra for help with PBMC and neutrophil isolation, Kaouther Chammam for technical assistance, and Philippe Robert for helpful discussions.

This work was supported by institutional funds from the CNRS, INSERM, and Aix-Marseille Université, and grants from the Association pour la Recherche contre le Cancer (A.L.); the Fondation de Recherche Médicale (A.G.); the CNRS programme Prise de Risques (M.P.); the region Provence-Alpes Côte d'Azur, France (O.T.); the UK Royal Society-CNRS Exchange Program (N.H. and A.L.); and the Investissements d'Avenir/Laboratoire d'Excellence INFORM program.

REFERENCES

1. von Andrian, U. H., and T. R. Mempel. 2003. Homing and cellular traffic in lymph nodes. *Nat. Rev. Immunol.* 3:867–878.
2. Ley, K., C. Laudanna, ..., S. Nourshargh. 2007. Getting to the site of inflammation: the leukocyte adhesion cascade updated. *Nat. Rev. Immunol.* 7:678–689.
3. Evans, R., I. Patzak, ..., N. Hogg. 2009. Integrins in immunity. *J. Cell Sci.* 122:215–225.
4. Schenkel, A. R., Z. Mamdouh, and W. A. Muller. 2004. Locomotion of monocytes on endothelium is a critical step during extravasation. *Nat. Immunol.* 5:393–400.
5. Lämmermann, T., and M. Sixt. 2009. Mechanical modes of 'amoeboid' cell migration. *Curr. Opin. Cell Biol.* 21:636–644.
6. Sumagin, R., and I. H. Sarelius. 2010. Intercellular adhesion molecule-1 enrichment near tricellular endothelial junctions is preferentially associated with leukocyte transmigration and signals for reorganization of these junctions to accommodate leukocyte passage. *J. Immunol.* 184:5242–5252.
7. Culver, J. C., and M. E. Dickinson. 2010. The effects of hemodynamic force on embryonic development. *Microcirculation.* 17:164–178.
8. Zhu, J., B. H. Luo, ..., T. A. Springer. 2008. Structure of a complete integrin ectodomain in a physiologic resting state and activation and deactivation by applied forces. *Mol. Cell.* 32:849–861.
9. Alon, R., and M. L. Dustin. 2007. Force as a facilitator of integrin conformational changes during leukocyte arrest on blood vessels and antigen-presenting cells. *Immunity.* 26:17–27.
10. Coughlin, M. F., and G. W. Schmid-Schönbein. 2004. Pseudopod projection and cell spreading of passive leukocytes in response to fluid shear stress. *Biophys. J.* 87:2035–2042.
11. Moazzam, F., F. A. DeLano, ..., G. W. Schmid-Schönbein. 1997. The leukocyte response to fluid stress. *Proc. Natl. Acad. Sci. USA.* 94:5338–5343.
12. Cinamon, G., V. Shinder, and R. Alon. 2001. Shear forces promote lymphocyte migration across vascular endothelium bearing apical chemokines. *Nat. Immunol.* 2:515–522.
13. Woolf, E., I. Grigorova, ..., R. Alon. 2007. Lymph node chemokines promote sustained T lymphocyte motility without triggering stable integrin adhesiveness in the absence of shear forces. *Nat. Immunol.* 8:1076–1085.
14. Schreiber, T. H., V. Shinder, ..., R. Sackstein. 2007. Shear flow-dependent integration of apical and subendothelial chemokines in T-cell transmigration: implications for locomotion and the multistep paradigm. *Blood.* 109:1381–1386.
15. Auffray, C., D. Fogg, ..., F. Geissmann. 2007. Monitoring of blood vessels and tissues by a population of monocytes with patrolling behavior. *Science.* 317:666–670.
16. Phillipson, M., B. Heit, ..., P. Kubas. 2009. Vav1 is essential for mechanotactic crawling and migration of neutrophils out of the inflamed microvasculature. *J. Immunol.* 182:6870–6878.
17. Sumagin, R., H. Prizant, ..., I. H. Sarelius. 2010. LFA-1 and Mac-1 define characteristically different intraluminal crawling and emigration patterns for monocytes and neutrophils in situ. *J. Immunol.* 185:7057–7066.
18. Ding, Z. M., J. E. Babensee, ..., C. M. Ballantyne. 1999. Relative contribution of LFA-1 and Mac-1 to neutrophil adhesion and migration. *J. Immunol.* 163:5029–5038.
19. Rainger, G. E., C. D. Buckley, D. L. Simmons, and G. B. Nash. 1999. Neutrophils sense flow-generated stress and direct their migration via $\alpha_v\text{-}\beta_3$ integrin. *Am. J. Physiol.* 276:H858–H864.
20. Smith, L. A., H. Aranda-Espinoza, ..., D. A. Hammer. 2007. Interplay between shear stress and adhesion on neutrophil locomotion. *Biophys. J.* 92:632–640.
21. Bartholomäus, I., N. Kawakami, ..., A. Flügel. 2009. Effector T cell interactions with meningeal vascular structures in nascent autoimmune CNS lesions. *Nature.* 462:94–98.
22. Steiner, O., C. Coisne, ..., R. Lyck. 2010. Differential roles for endothelial ICAM-1, ICAM-2, and VCAM-1 in shear-resistant T cell arrest, polarization, and directed crawling on blood-brain barrier endothelium. *J. Immunol.* 185:4846–4855.
23. Lipowsky, H. H., S. Kovalchek, and B. W. Zweifach. 1978. The distribution of blood rheological parameters in the microvasculature of cat mesentery. *Circ. Res.* 43:738–749.

24. Koutsiaris, A. G., S. V. Tachmitzi, ..., D. Z. Chatzoulis. 2007. Volume flow and wall shear stress quantification in the human conjunctival capillaries and post-capillary venules in vivo. *Biorheology*. 44:375–386.
25. Granger, D. N., and P. Kubes. 1994. The microcirculation and inflammation: modulation of leukocyte-endothelial cell adhesion. *J. Leukoc. Biol.* 55:662–675.
26. Johnston, B., T. B. Issekutz, and P. Kubes. 1996. The α 4-integrin supports leukocyte rolling and adhesion in chronically inflamed postcapillary venules in vivo. *J. Exp. Med.* 183:1995–2006.
27. Xu, H., A. Manivannan, ..., I. J. Crane. 2004. Reduction in shear stress, activation of the endothelium, and leukocyte priming are all required for leukocyte passage across the blood—retina barrier. *J. Leukoc. Biol.* 75:224–232.
28. Perry, M. A., and D. N. Granger. 1991. Role of CD11/CD18 in shear rate-dependent leukocyte-endothelial cell interactions in cat mesenteric venules. *J. Clin. Invest.* 87:1798–1804.
29. Edelstein, A., N. Amodaj, K. Hoover, R. Vale, and N. Stuurman. 2010. Computer control of microscopes using microManager. *Curr. Protoc. Mol. Biol.* Unit 14.20.
30. Moghe, P. V., R. D. Nelson, and R. T. Tranquillo. 1995. Cytokine-stimulated chemotaxis of human neutrophils in a 3-D conjoined fibrin gel assay. *J. Immunol. Methods.* 180:193–211.
31. Palecek, S. P., J. C. Loftus, ..., A. F. Horwitz. 1997. Integrin-ligand binding properties govern cell migration speed through cell-substratum adhesiveness. *Nature*. 385:537–540.
32. Abraham, V. C., V. Krishnamurthi, ..., F. Lanni. 1999. The actin-based nanomachine at the leading edge of migrating cells. *Biophys. J.* 77:1721–1732.
33. Marcy, Y., J. Prost, ..., C. Sykes. 2004. Forces generated during actin-based propulsion: a direct measurement by micromanipulation. *Proc. Natl. Acad. Sci. USA.* 101:5992–5997.
34. Dalous, J., E. Burghardt, ..., T. Bretschneider. 2008. Reversal of cell polarity and actin-myosin cytoskeleton reorganization under mechanical and chemical stimulation. *Biophys. J.* 94:1063–1074.
35. Rivière, C., S. Marion, ..., C. Wilhelm. 2007. Signaling through the phosphatidylinositol 3-kinase regulates mechanotaxis induced by local low magnetic forces in *Entamoeba histolytica*. *J. Biomech.* 40:64–77.
36. Weber, G. F., M. A. Bjerke, and D. W. DeSimone. 2012. A mechanoresponsive cadherin-keratin complex directs polarized protrusive behavior and collective cell migration. *Dev. Cell.* 22:104–115.
37. Zaidel-Bar, R., Z. Kam, and B. Geiger. 2005. Polarized downregulation of the paxillin-p130CAS-Rac1 pathway induced by shear flow. *J. Cell Sci.* 118:3997–4007.
38. Goel, S., D. G. Duda, ..., R. K. Jain. 2011. Normalization of the vasculature for treatment of cancer and other diseases. *Physiol. Rev.* 91:1071–1121.